Clinical and Translational Radiation Oncology 26 (2021) 15–23

Contents lists available at ScienceDirect

Clinical and Translational Radiation Oncology

journal homepage: www.elsevier.com/locate/ctro

Original Research Article

# Dacomitinib and gedatolisib in combination with fractionated radiation in head and neck cancer

George D. Wilson [a,*], Thomas G. Wilson [a], Alaa Hanna [a], Mohamad Dabjan [a], Katie Buelow [a], John Torma [a], Brian Marples [b], Sandra Galoforo [a]

[a] Department of Radiation Oncology, William Beaumont Hospital, Royal Oak, MI, United States
[b] Department of Radiation Oncology, University of Rochester, Rochester, NY, United States

ARTICLE INFO

*Article history:*
Received 13 August 2020
Revised 2 November 2020
Accepted 3 November 2020
Available online 8 November 2020

*Keywords:*
Head and neck cancer
Radiation
Targeted agents
Xenografts
Growth delay

ABSTRACT

*Background and purpose:* There has been little success targeting individual genes in combination with radiation in head and neck cancer. In this study we investigated whether targeting two key pathways simultaneously might be more effective.

*Materials and methods:* We studied the effect of combining dacomitinib (pan-HER, irreversible inhibitor) and gedatolisib (dual PI3K/MTOR inhibitor) with radiation in well characterized, low passage xenograft models of HNSCC in vitro and *in vivo*.

*Results:* Dacomitinib showed differential growth inhibition in vitro that correlated to EGFR expression whilst gedatolisib was effective in both cell lines. Neither agent radiosensitized the cell lines in vitro. In vivo studies demonstrated that dacomitinib was an effective agent alone and in combination with radiation whilst the addition of gedatolisib did not enhance the effect of these two modalities despite inhibiting phosphorylation of key genes in the PI3K/MTOR pathway.

*Conclusions:* Our results showed that combining two drugs with radiation provided no added benefit compared to the single most active drug. Dacomitinib deserves more investigation as a radiation sensitizing agent in HNSCC.



## 1. Background and significance

The *EGFR/PI3K/AKT/mTOR* signaling pathway plays a central role in numerous important cellular processes, including growth, proliferation, differentiation, migration, inflammation and survival under normal physiological and pathophysiological conditions such as cancer [1]. Genomic characterization of head and neck squamous cell cancer (HNSCC) has identified mutations in many genes that converge on the *EGFR/RAS/RAF/ERK/PI3K/AKT/mTOR* signaling cascade [2,3] and molecular alterations in one or more components of this pathway are present in more than 80% of HNSCC [4,5]. As a result, this signaling pathway is considered to be a very attractive target for molecular-orientated therapy [6]. However, apart from the inhibitors of *EGFR* and vascular endothelial growth factor (*VEGF*), very few molecular targeted agents have advanced to phase III clinical trials in combination with radiation in HNSCC [7].

The early promise of cetuximab in combination with radiation in HNSCC [8] was not strengthened by a subsequent randomized trial that included cisplatin [9] that did not improve outcome. However, the drug remains important for locally advanced elderly patients who cannot tolerate cisplatin and in recurrent or metastatic disease [10]. Resistance to cetuximab has been associated with a dysregulation of normal EGFR recycling followed by increased human epidermal growth factor receptor 2 and 3 (HER2 and HER3) dimerization [11], the presence of the EGFR variant 3 (EGFRvIII) truncation mutation [12] and the presence of KRAS mutations [13]. The cooperation and signaling redundancy that exists between members of the HER family has been shown to maintain the activity of common downstream pathways despite inhibition of EGFR by cetuximab. In this study, we have used dacomitinib which is an orally active, second generation, highly selective, small-molecule pan-HER inhibitor [14] that has shown superiority over cetuximab in inhibiting growth of HNSCC cell lines [15] and has demonstrated additivity in combination with radiation with no apparent additional toxicity in a HNSCC xenograft model [16]. In a phase II study of dacomitinib in platinum-refractory recurrent or metastatic HNSCC, 10 patients (21%)

* Corresponding author at: William Beaumont Hospital, Department of Radiation Oncology, 3811 W Thirteen Mile Road, Royal Oak, Michigan 48073, United States.
*E-mail address:* george.wilson@beaumont.edu (G.D. Wilson).

https://doi.org/10.1016/j.ctro.2020.11.003

exhibited a partial response and 31 (65%) achieved stable disease. The drug was well tolerated, with the most common adverse events being low-grade skin toxicity or diarrhea [17].

Although targeting EGFR is still considered the most attractive route for radiosensitizing HNSCC, the lack of success of studies targeting individual genes is likely due to the complexity of the signaling pathways in cancer where there are multiple nodes, feedback loops, crosstalk and redundancy. To overcome these issues it would seem rational that targeting these pathways at several points simultaneously might be more effective [18,19]. It has been reported that activation of downstream survival pathways leads to resistance to EGFR inhibitors. Of these downstream pathways, deregulation of PI3K/AKT/MTOR signaling has been identified as important determinant of radiosensitivity in HNSCC [18,20,21]. Several studies have investigated the utility of different PI3K/MTOR inhibitors in various experimental settings in HNSCC both in vitro and *in vivo* [22–28]. However, only a few studies report the efficacy of the combination of PI3K inhibitors in combination with radiation [22,27,28]. In this study we have used gedatolisib (PF-05212384, PKI-587) which is a highly potent dual inhibitor of PI3Kα, PI3Kγ and mTOR [29]. Importantly, we have studied whether dual inhibition with dacomitinib and gedatolisib further enhances the radiation response.

## 2. Materials and methods

### 2.1. Cell lines and drugs

The UT-SCC cell lines were provided by Dr. Reidar Grénman (Turku University Hospital, Turku, Finland). All are from a series of HPV-negative cell lines which were developed from primary and recurrent HNSCC specimens during the 1990s [30,31]. These cell lines have been maintained at low passage number (<20) and we have used these cell lines extensively in a number of studies where the cell lines, and xenografts obtained from them, have maintained consistent and reproducible characteristics [32–43]. In addition, other researchers have utilized these cell lines [44–50] and shown similar radiation responses and other characteristics to those reported in our studies. Cells were cultured and maintained in Dulbecco's modified Eagle's medium supplemented with 10% fetal bovine serum, penicillin (100 U/ml), and streptomycin (100 mg/ml) and maintained at low passage number. Dacomitinib and gedatolisib was kindly provided by Pfizer (NY, USA). A 10 mM solution of each was prepared in dimethyl sulfoxide and stored at −70 °C for in vitro experiments.

### 2.2. Irradiation

Cells were irradiated with an Xstrahl X-ray System, Model RS225 (Xstrahl, UK) at a dose rate of 0.29 Gy/min, tube voltage of 160 kVp, current of 4 mA and filtration with 0.5 mM Al and 0.5 mM Cu. Cells were irradiated (0.5–4 Gy) in 25 $cm^2$ flasks at 37 °C. Animals were irradiated with a Faxitron Cabinet X-ray System, Model 43855F (Faxitron X-Ray, Wheeling, IL, USA) at a dose rate of 0.69 Gy/min, tube voltage of 160 kVp and current of 4 mA.

### 2.3. 3-(4, 5-Dimethylthiazol-2yl)-2, 5-diphenyltetrazolium bromide (MTT) assay

For the MTT assay, cells were plated into 96 well plates and allowed to attach overnight. The following day, media were exchanged for media containing various concentrations of dacomitinib or gedatolisib and the plates returned to the incubator. Control cultures contained media with appropriate DMSO concentration. After an additional 3 days, MTT (5 mg/ml PBS) was added to each well and the plate returned to the $CO_2$ incubator for 5 h. The media/MTT was then aspirated from the wells and DMSO was added to dissolve the purple formazan. After 5 min incubation at 37 °C, absorbance readings (at 560 nm and 670 nm) were taken on a Versamax multiplate reader (Molecular Devices, Sunnyvale, CA).

### 2.4. Clonogenic survival assay

Cells were plated into T25 flasks at different dilutions depending on the dose of radiation such that a significant number of colonies would be scored at the end of the experiment. The timings of drug administration relative to radiation were determined using the MTT assay (data not shown) to establish the optimal scheduling. At 2 h prior to irradiation, media was exchanged for media containing 5 nM Gedatolisib. At 1 h prior to irradiation, media was exchanged for media containing 7.5 nM Dacomitinib. Control cells had media exchanged for normal media containing the appropriate DMSO concentration. Cells were then irradiated (0–4 Gy) and plated into flasks that contained the same media/drug that the cells had been in. Colonies were allowed to develop for 10–14 days. The colonies (~50 cells) were then stained with crystal violet, counted and surviving fractions were calculated. Data was normalized for plating efficiency and survival curves were fitted using the linear-quadratic equation.

### 2.5. Flow cytometric analysis of gamma-H2AX (γH2AX) and cell cycle

Cells plated into T25 flasks and allowed to grow for 3 days. One hour prior to radiation treatment, media was exchanged for media +10 nM Dacomitinib (37 °C) or media only with DMSO (37 °C) and returned to the incubator. For γH2AX assessment, after one hour, flasks were irradiated with 2 Gy at 37 °C and then returned to the incubator. Cells were collected at 0, 1, 2, 4, 6 and 24 h post irradiation. Cells were trypsinized, washed twice with PBS and then fixed with 70% ETOH. Cell cycle analysis was studied without the addition of radiation. Samples were stored at −20 °C until analysis.

For γH2AX analysis, fixed cells were pelleted and then permeabilized with 1%Triton X-100. Cells were washed with PBS + Tween 20(PBT) and blocked for one hour with PBT + 3% BSA. After blocking, cells were washed 2 times with PBT and then incubated with Anti-Phospho-Histone H2A.X antibody (cloneJBW301) (Millipore Sigma, Burlington, MA) for 1 h. After incubation, cells washed 2 times with PBT and then incubated with secondary antibody, Goat anti-mouse IgG1-Alexa Fluor 488(Invitrogen, Carlsbad, CA), for 1 h. Cells were washed 3 times and resuspended in PBT. Flow cytometric analysis was performed on FACS Canto II (BD Biosciences, San Jose, CA). The mean fluorescence values were recorded for the total cell population in each sample. The data was calculated by normalizing the treated samples to the mean fluorescent of the control samples.

For cell cycle analysis $10^6$ cells were resuspended in 1 ml of PBT containing 1 mg/ml RNAse A (Millipore Sigma) and 10 μg/ml propidium iodide (Millipore Sigma). Flow cytometric analysis was performed on FACS Canto II (BD Biosciences, San Jose, CA) and cell cycle analysis performed using ModFitLT (Verity Software House, Topsham, ME).

### 2.6. Xenograft growth delay assay

All animal experiments were approved by the Institute Animal Care and Use Committee. Xenografts were established in 4–6 week old female nude NIH III mice (Charles Rivers Laboratories, Wilmington, MA) by injecting UT-SCC-14 subcutaneously into the flank, at a density of $2x10^6$ cells per 100 μl Matrigel (Corning, Corning, NY) or UT-SCC-15 at a density of $4 \times 10^6$ per 100 μl Matrigel.

Tumor volume was measured twice weekly by digital calipers and calculated using the formula (πab2)/6, where a = largest diameter, b = smallest diameter). Mice were randomly assigned to experimental groups once the tumors reached a volume of 200–300 $mm^3$. Experimental endpoint is tumor volume of 2000 $mm^3$ or 160 days post end of treatment.

The UT-14-SCC xenograft assay consisted of eight treatment groups: (1) control, no drugs, no RT, (2) RT delivered as 2.0 Gy/day(5 times/week) for three weeks (3) dacomitinib (10 mg/kg), oral gavage daily(5 times/week) for 3 weeks, (4) dacomitinib + RT, dacomitinib by oral gavage, 1 h prior to RT (5 times/week) for 3 weeks, (5) gedatolisib (6 mg/kg), i.v., 2 times/week (M&Th) for 3 weeks, (6) gedatolisib + RT, gedatolisib, i.v., 2 h prior to radiation 2 times/week (M&Th), (7) dacomitinib (as N group 3) + gedatolisib (as in group 5), gedatolisib administered 1 h prior to dacomitinib on M and Th, dacomitinib only T, W and F for 3 weeks, (8) dacomitinib + gedatolisib + RT. The vehicle for dacomitinib was 0.5% methylcellulose and the volume was 0.1 cc. The vehicle for gedatolisib was 5% dextrose, 0.25% lactic acid solution in a volume of 0.15 cc.

For UT-15-SCC xenografts, the treatment groups and drug concentrations were the same but the radiation dose per fraction was increased to 3 Gy as the UT-15-SCC cells are more radioresistant than the UT-14-SCC.

### 2.7. Western immunoblot assay

Protein expression was analyzed in xenograft tumor tissue after treatment. Two mice from each treatment arm and each tumor model were sacrificed at the end of the three week treatment period and snap-frozen. Cellular protein was extracted from the frozen material with a SDS protein lysis buffer and stored at −20 °C. For the extraction of protein, a small piece of tumor was homogenized in T-PER (ThermoFisher-Scientific, Waltham, MA) with Halt protease/phosphatase inhibitor (ThermoFisher-Scientific, Waltham, MA) added. Unsolubilized tissue was centrifuged out and the supernatant was collected and stored at −70 °C. Equal amounts of protein (20 μg) were separated by 10% sodium dodecyl sulfate polyacrylamide gel electrophoresis and transferred onto a nitrocellulose membrane by electroblotting. After blocking, the membrane was incubated with primary antibody overnight at 4 °C. The following primary antibodies were obtained from Cell Signaling Technology (Danvers, MA)., pan AKT(clone 11E7 catalog #46855)), Phospho-AKT (Ser473) (clone D25E6 catalog #130385), PI3 Kinase p110α (clone D5585 catalog #5405), Phospho-PI3 Kinase p85(Tyr458)/p55(Tyr199) (catalog #42285), 4E-BP1(clone 53H11 catalog #9644), Phospho-4E-BP1(Thr37/46) (clone 236B4 catalog # 2855), S6 Ribosomal Protein (clone 54D2 catalog # 2217), Phospho-S6 Ribosomal Protein(Ser240/244) (clone D68F8 catalog # 5364), p44/42 MAPK (clone 137F5 catalog # 4695), Phospho-p44/p42 MAPK (Thr202/Tyr204) (clone 197G2 catalog # 4377), EGF Receptor (clone D38B1 catalog # 54359), and Phospho-EGF Receptor(Tyr992) (catalog # 2235) (Actin (MP Biomedicals, Irvine, CA). The membrane was washed and the secondary antibody (IRDye 800CW, Licor, Lincoln, NB) was applied for 1 h at room temperature. The membranes were analyzed with an Odyssey infra-red imaging system (Li-Cor, Lincoln, NB). Absorbance data was normalized to the actin band for each gel and then calculated as a fold change compared to untreated controls.

### 2.8. Statistical analysis

In vitro experiments were repeated three times and statistical analysis was carried out using a two-way t-test or one-way analysis of variance. Data are presented as the mean ± SE. A probability level of a p-value of $< 0.05$ was considered significant. In vivo growth delay data was analyzed based on a time-to-event analysis, i.e. the time to reach 3 times initial volume. Differences between treatment groups were analyzed using a one-way ANOVA and a Tukey post hoc test was then performed between each group comparison, $p < 0.05$ was considered statistically significant. Animals sacrificed prior to reaching tumor volume endpoint due to predetermined animal welfare criteria (as per protocol) were censored at the time of euthanasia.

## 3. Results

### 3.1. Dacomitinib is a potent inhibitor in EGFR overexpressing cell lines

Dacomitinib showed potent inhibition of the UT-SCC-14 cell line with and $IC_{50}$ of 0.0023 μM (Fig. 1B). This cell line has a high level of EGFR overexpression (Fig. 1A).

A pattern of sensitivity emerged showing an inverse correlation with EGFR overexpression for three other cells lines UT-SCC-15 ($IC_{50}$ of 0.72 μM), UT-SCC-16 ($IC_{50}$ of 0.48 μM) and UT-SCC24A ($IC_{50}$ of 0.16 μM) (Fig. 1A + B).

### 3.2. Gedatolisib is effective irrespective of EGFR status

Two cell lines at the different ends of the dacomitinib activity spectrum, UT-SCC-14 and UT-SCC-15, were selected and exposed to different concentrations of gedatolisib (Fig. 1C). The drug had similar activity in both cell lines with an $IC_{50}$ of 0.0062 μM in UT-SCC-14 and $IC_{50}$ of 0.019 μM in UT-SCC-15.

### 3.3. Neither drug modifies the radiation response in vitro

Concentrations of dacomitinib and gedatolisib that produced significant growth inhibition were combined with graded doses of radiation both alone and in combination. There was no effect of the drugs on the radiation response in UT-SCC-14 (Fig. 2A) whilst in UT-SCC-15 there was a trend for dacomitinib, with or without gedatolisib, to be radioprotective although this was not significant (Fig. 2B).

### 3.4. γ-H2AX staining and cell cycle analysis

To further study the observations obtained in the clonogenic assays, UT-SCC-14 and UT-SCC-15 cell lines were irradiated with 2 Gy with or without 10 nm dacomitinib and assayed for γ-H2AX staining using flow cytometry (Fig. 2C and D). The cell lines differ in their radiosensitivity in vitro (Fig. 2 A and B). These differences were also apparent in Fig. 2C and D where the γ-H2AX fluorescent staining intensity was greater in UT-SCC-14 signifying more DNA double strand breaks (DSB) that peaked at 2 h with evidence of unrepaired DSBs at 24 h. In contrast UT-SCC-15 showed a modest increase in staining and was completely resolved at 24 h. Dacomitinib had only a minor effect on the radiation-induced γ-H2AX response in UT-SCC-14 but repressed the response in UT-SCC-15 (Fig. 3D).

Dacomitinib had a more profound effect on the cell cycle of UT-SCC-14 compared to UT-SCC-15 (Fig. 2E and F). There was little change in cell cycle distribution during the first 6 h but by 24 h there was an accumulation in G1 and reduction in S-phase which was more pronounced in UT-SCC-14 cells.

### 3.5. Effect of drugs and radiation on tumor growth and survival

The effect of the drugs and radiation are shown in Fig. 3. For clarity the data is shown for each drug and their combination as

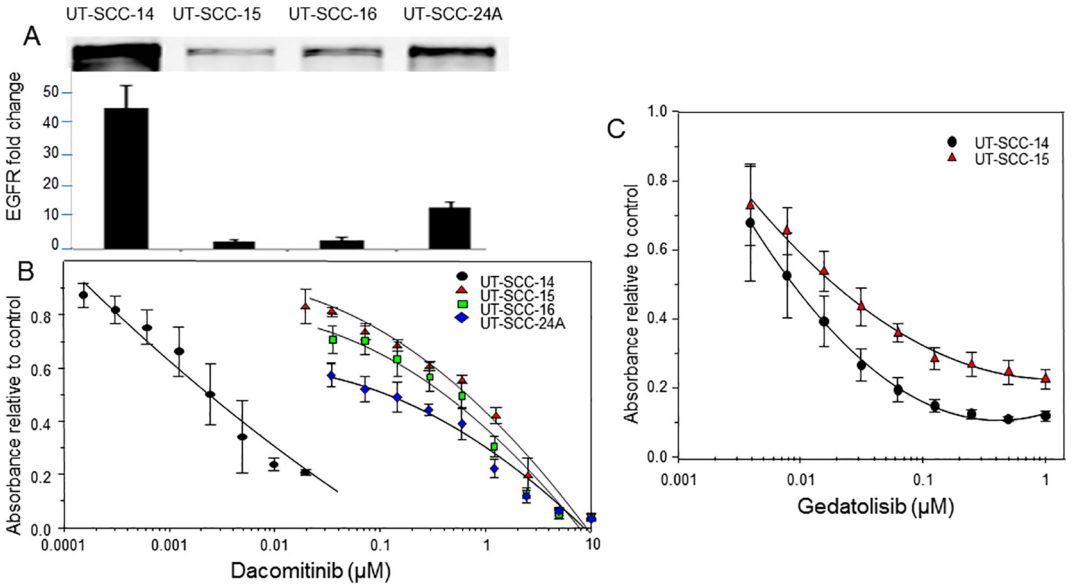


**Fig. 1.** The effect of dacomitinib and gedatolisib on cell viability of HNSCC cell lines in vitro. In panel A western blots for EGFR expression are shown for four different HNSCC cell lines. In panel B, the effect of different concentrations of dacomitinib on cell viability of these cell lines is presented (n = 3 replicates, the error bars were excluded for clarity). In panel C, the effect of gedatolisib was studied in the most sensitive and most resistant cell lines to dacomitinib (n = 3 replicates).

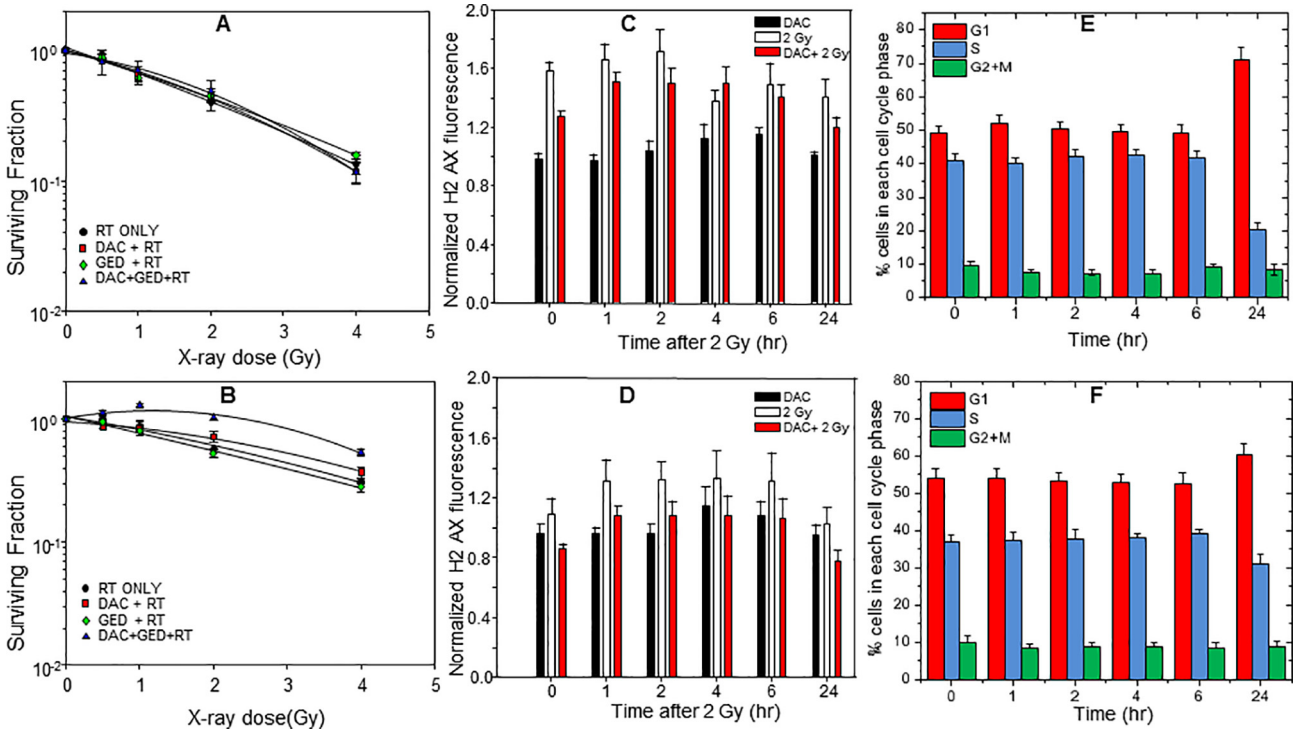


**Fig. 2.** Neither dacomitinib (A) or gedatolisib (B) sensitizes UT-SCC-14 or 15 cells to radiation in vitro. Dacomitinib does not enhance DNA double strand breaks induced by 2 Gy of radiation in UT-SCC-14 (C) or UT-SCC-15 (D). Dacomitinib causes a substantial accumulation of cells in the G1 phase of the cell cycle in UT-SCC-14 cells (E) but has less effect in UT-SCC-15 (F). All experiments were repeated three times with an n = 3.

separate growth curves such that the control and radiation alone arm is repeated in each graph. The growth delay data is presented in Table 1 as the time to reach three times the initial volume at the start of treatment; each mouse has been normalized to its individual starting volume. The mean starting volume ranged from 285 $mm^3$ to 364 $mm^3$ across the eight treatment groups in UT-SCC-14 and from 162 $mm^3$ to 242 $mm^3$ in the UT-SCC-15 treatment groups.

Taking each agent into consideration, gedatolisib was ineffective in UT-SCC-14 xenografts both as a single agent and in combination with RT (Fig. 3B, Tables 1 and 2). In contrast this agent resulted in significant growth inhibition in the UT-SCC-15 xenograft ($p = 0.0395$) (Fig. 3E) but appeared to reduce the effect of radiation when the two modalities were combined. Radiation caused a growth delay of 132.2 days whilst this was reduced to 100.3 days in the presence of gedatolisib ($p = 0.005$).

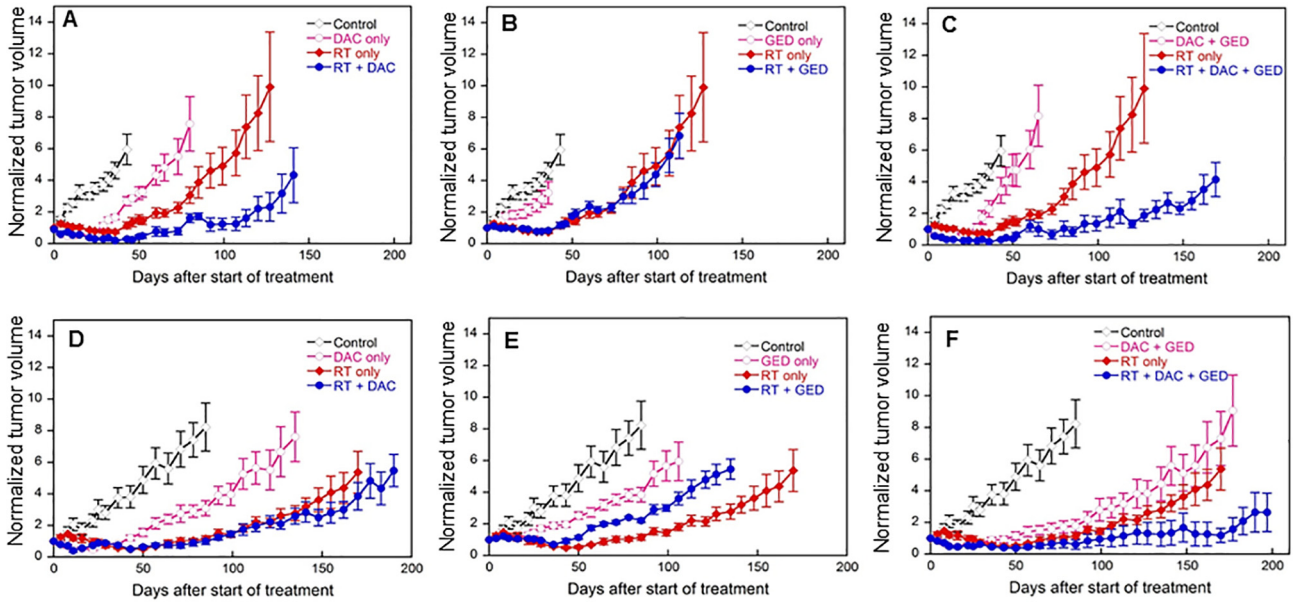


**Fig. 3.** The effect of dacomitinib and gedatolisib alone and in combination with fractionated radiation on UT-SCC-14 and 15 xenografts. In each graph the symbols represent controls (◇), drug alone (○), radiation alone (◆) and drug(s) plus radiation (●). It should be noted that all experimental studies with the drugs and radiation were performed simultaneously such that the control and radiation alone curves are the same in each drug treatment but have been separated for each drug and their combination for clarity: n = 5 for all treatments.

**Table 1**
Growth delay measured as time to reach three times the pre-treatment starting volume. Each individual tumor was normalized to its starting volume and the data are presented as mean ± S.E.M.

| Treatment | Time to reach 3 times pre-treatment volume (days) | |
|---|---|---|
| | UT-SCC-14 | UT-SCC-15 |
| Control | 9.0 ± 1.7 | 33.3 ± 5.8 |
| DAC | 38.8 ± 1.5 | 87.7 ± 9.9 |
| GED | 16.3 ± 2 0.7 | 70.4 ± 10.6 |
| DAC + GED | 37.5 ± 4.5 | 96.0 ± 6.5 |
| RT | 59.0 ± 2.6 | 132.2 ± 4.2 |
| DAC + RT | 137.9 ± 15.3 | 156.0 ± 13.2 |
| GED + RT | 64.4 ± 5.2 | 100.3 ± 4.6 |
| DAC + GED + RT | 139.8 ± 9.2 | 176.4 ± 17.4 |

**Table 2**
Statistical comparison of the treatments and their combinations. The numbers represent p-values with significant differences highlighted in bold.

| Treatment | Time to reach 3 times pre-treatment volume (days) | |
|---|---|---|
| | UT-SCC-14 | UT-SCC-15 |
| Control vs. DAC only | **0.0003** | **0.0027** |
| Control vs. GED only | 0.0864 | **0.0395** |
| Control vs. combo | **0.0215** | **0.0011** |
| Control vs. RT only | **0.0006** | **>0.0001** |
| Control vs. RT + DAC | **0.0020** | **0.0029** |
| Control vs. RT + GED | **0.0006** | **>0.0001** |
| Control vs. RT + combo | **0.0050** | **0.0013** |
| DAC only vs. GED only | **0.0041** | 0.3099 |
| DAC only vs. combo | 0.6346 | 0.5479 |
| GED only vs. combo | 0.0765 | 0.1366 |
| Combo vs. RT only | **0.0231** | **0.0159** |
| RT only vs. DAC + RT | **0.0106** | 0.2707 |
| RT only vs. GED + RT | 0.3229 | **0.0050** |
| RT only vs. combo + RT | **0.0119** | 0.0986 |
| DAC + RT vs. GED + RT | **0.0181** | **0.0438** |
| DAC + RT vs. combo + RT | 0.9153 | 0.4740 |
| GED + RT vs. combo + RT | **0.0148** | **0.0188** |

Dacomitinib was active in both xenograft models causing significant growth delay as a single agent (Fig. 3A and D, Tables 1 and 2). When combined with radiation, there was significant prolongation of growth delay in the UT-SCC-14 model compared to RT alone (Table 2) and 3 of 5 animals had no detectable tumor at the end of the observation period of 160 days. In the more slowly growing UT-SCC-15 model, none of the animals treated with dacomitinib and RT had reached sacrifice criteria at 200 days.

When the two agents were used in combination with or without RT, their combined effects mirrored the effect of each agent alone (Fig. 3C and E) and their combination with radiation produced no further growth delay than seen with dacomitinib and radiation without gedatolisib.

### 3.6. Immunoblotting

A separate subset of mice was sacrificed at the end of the three week treatment period to assess the status of key proteins involved in the pathways targeted by the drugs. Fig. 4A and B shows the blots obtained for all combinations of treatments on the expression of the two of the major proteins in the EGFR/RAS/RAF/MAPK pathway whilst Fig. 5A and B shows the blots obtained on the expression major proteins involved in the AKT/PI3K/MTOR pathway. Quantitative data for phosphoprotein expression is presented in Supplemental Table 1.

Radiation alone had minor effects on the phosphorylated proteins in both signaling pathways (Figs. 4 and 5 and Table 3)

Dacomitinib had little effect on total EGFR or MAPK levels but downregulated p-EGFR and p-MAPK in both tumor models (Fig. 4A and B). When combined with RT, the effect on p-EGFR and p-MAPK was marginally greater (Table 3). Gedatolisib did not alter EGFR/MAPK signaling. The combination of dacomitinib and gedatolisib slightly diminished the effect of dacomitinib alone in both tumor models (Fig. 4, Table 3). When both drugs were combined with RT, the effect on p-EGFR and p-MAPK was similar to combination dacomitinib and RT in UT-SCC-14 but was not as effective as dacomitinib with RT in the UT-SCC-15 tumor model.

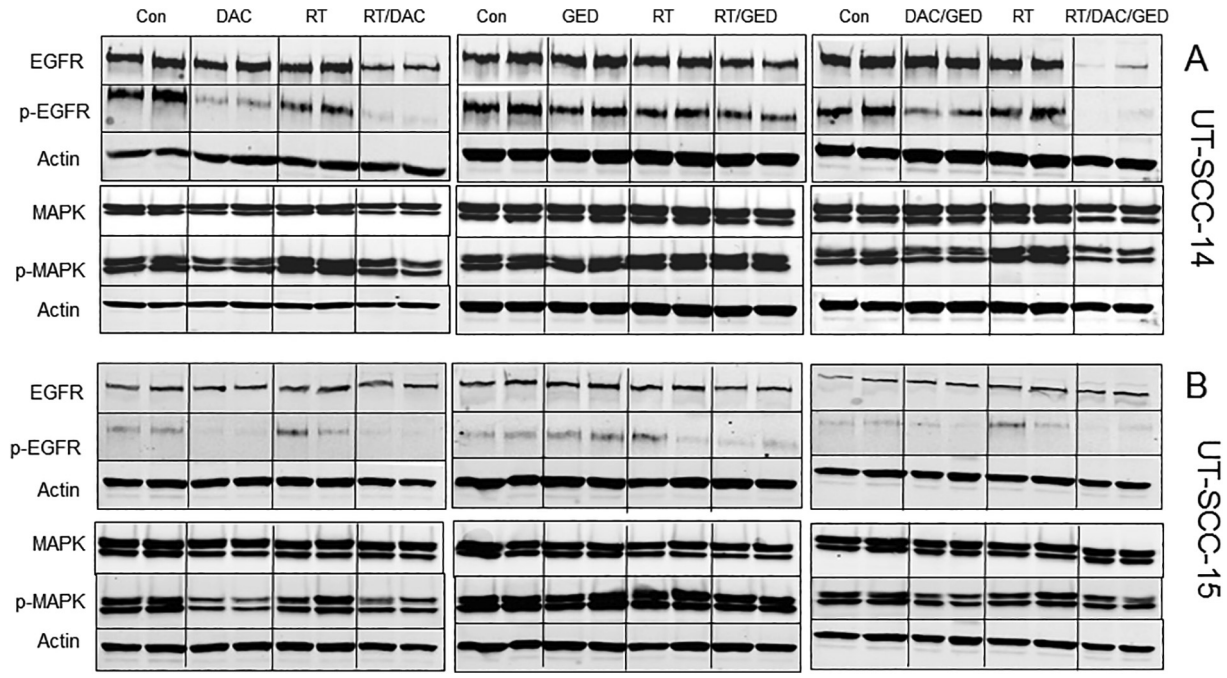


**Fig. 4.** Immunoblotting for each drug and combination with radiation in UT-SCC-14 xenografts (A) and UT-SCC-15 xenografts (B) for total and phoshorylated proteins in the EGFR pathway. Actin controls are shown for each gel (data not shown for clarity). There was n = 2 for these studies.

Dacomitinib was without effect on PI3K/AKT/MTOR signaling except for a significant reduction in p4EBP1 in the UT-SCC-14 tumor (Fig. 5A and B); its combination with RT was equally ineffective. Gedatolisib downregulated phosphorylation of proteins downstream of PI3K in both tumor models but the effect was more pronounced in UT-SCC-15 (Fig. 5A and B, Table 3). Combining gedatolisib with RT did not further enhance the downregulation of these phosphoproteins. The combination of all three agents was not any more effective than the gedatolisib alone at downregulating PI3K/AKT/MTOR pathway phosphoproteins. Radiation alone had minor effects on the phosphorylated proteins.

## 4. Discussion

Many studies have provided compelling pre-clinical evidence for the use of EGFR and PI3K pathway inhibitors to treat HNSCC [25,28,51–57]. Several of these studies have explored the combination of agents targeting both pathways with success in vitro [25,28,51,53]. However, very few studies have investigated dual targeting of these pathways in combination with radiation which remains standard-of-care in primary HNSCC. In a previous study we reported the combination of a MEK1/2 inhibitor (binimetinib) with a pan-PI3K inhibitor (buparlisib) and fractionated radiation in the same tumor models employed in this present study [42]. There were two unexpected findings from this previous study. First, the data showed discordance between the in vitro and *in vivo* data. Whereas buparlisib was equally effective in reducing growth of both cell lines in vitro, it had a much greater effect on UT-SCC-15 tumors while having little influence on the growth of UT-SCC-14. This was even more apparent with binimetinib which demonstrated high sensitivity against UT-SCC-14 cells in vitro compared to UT-SCC-15 but the *in vivo* data showed the opposite response. The second unexpected finding was that no significant benefit was gained by the combined use of the two agents with RT even though each was efficacious when used alone with radiation [42].

In this present study we obtained somewhat similar results. Again the in vitro data did not translate into the same effect *in vivo*. The UT-14-SCC cell line was exquisitely sensitive to dacomitinib with a 200-fold difference in response compared to UT-SCC-15 cells, yet both tumor models were responsive *in vivo* either with dacomitinib alone or in combination with RT. Gedatolisib showed a modest inhibition of growth in both tumor models.

Considering that both cell lines were very sensitive to gedatolisib in vitro (Fig. 1C), the *in vivo* effect was very disappointing (Fig. 3, Table 1). Although there was a significant downregulation of phosphorylation of PI3K/AKT/MTOR signaling proteins (Fig. 5) in both tumor models, the impact on growth was modest and there was no positive interaction with dacomitinib or RT. PI3K and MTOR both belong to the PI3K-related kinases (PIKK) superfamily and share structural domains which has led to the development of agents such as gedatolisib that target both kinases [58]. Dual inhibitors of PI3K and mTOR target the active sites of both holoenzymes, inhibiting the pathway both upstream and downstream of AKT, thus avoiding the problem of AKT activation following abolition of the mTORC1–S6K–IRS1 negative feedback loop [59]. Preclinical in vitro cell screenings with dual PI3K/MTOR inhibitors have suggested a broader efficacy across more genotypes compared with agents targeting only one component of the pathway [60,61]. Gedatolisib inhibits PI3Kα, PI3Kγ and MTOR and we have previously studied PF-04691502 which is an ATP-competitive PI3K(α/β/δ/γ)/MTOR dual inhibitor [37] and buparlisib [42], a specific pan-class I PI3K family inhibitor, in the same tumor models. PF-04691502 and buparlisib also reduced phosphorylation of key components of the PI3K/AKT/MTOR signaling pathway in both tumor models. When comparing the three agents, buparlisib alone was the most active agent in the UT-SCC-15 tumor model followed by gedatolisib whereas PF-04691502 was inactive. In the UT-SCC-14 tumor model, buparlisib was inactive whereas the two dual PI3K/MTOR inhibitors showed modest activity at the doses used. In the context of radiation treatment only PF-04691502 [37] was able to significantly enhance the radiation response in UT-SCC-14

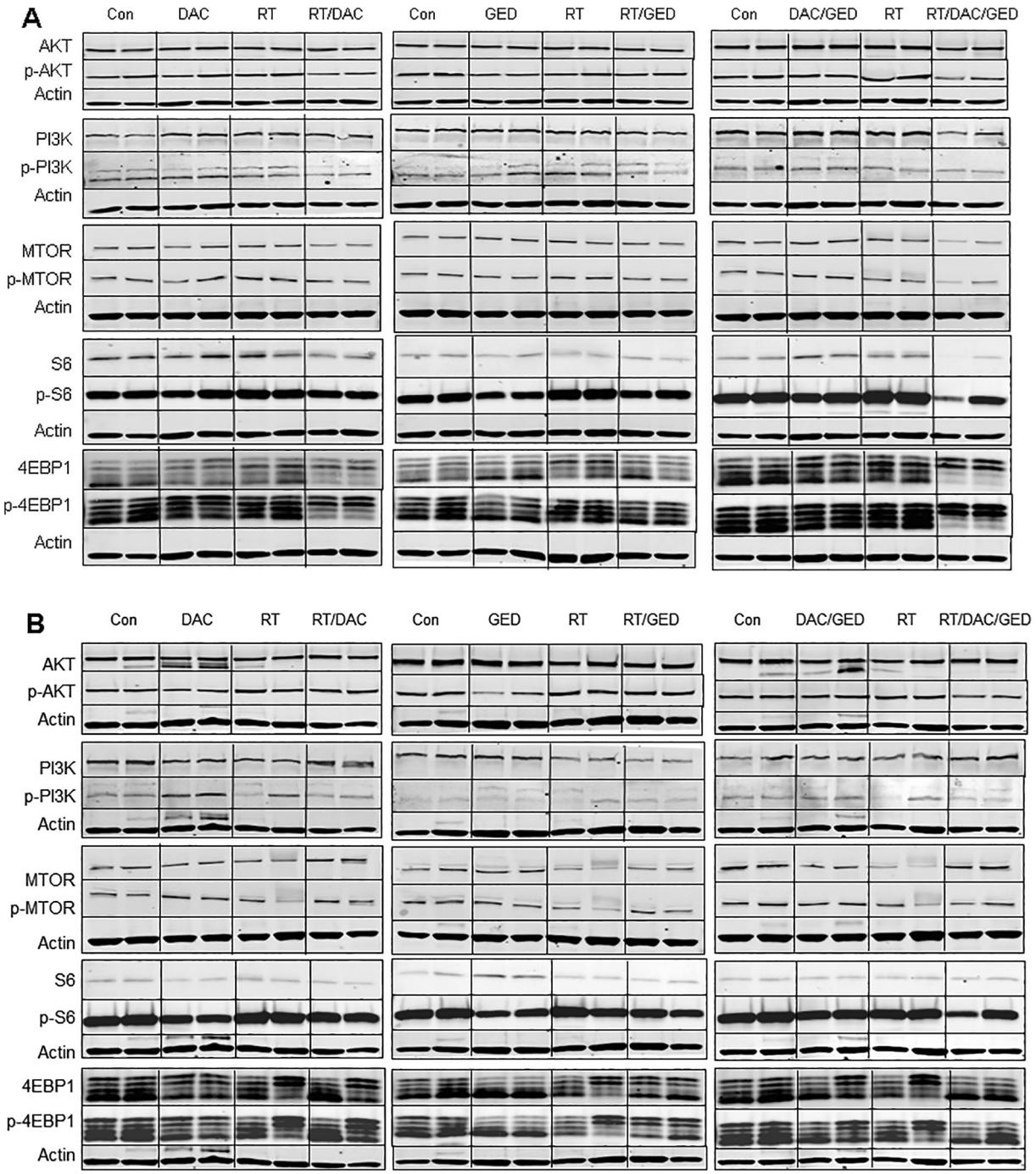


**Fig. 5.** Immunoblotting for each drug and combination with radiation in UT-SCC-14 xenografts (A) and UT-SCC-15 xenografts (B) for total and phoshorylated proteins in the PI3K pathway. Actin controls are shown for each gel (data not shown for clarity). There was n = 2 for these studies.

whilst buparlisib [42] was the only active radiation enhancer in UT-SCC-15. In this present study gedatolisib appeared to diminish the radiation effect in this tumor model (Fig. 3, Table 1). To an extent, the growth delay data mirrored the pathway inhibition analysis where our previous research showed that PF-04691502 was very effective agent at reducing phosphorylation AKT, S6 and 4EBP1 in UT-SCC-14 in combination with radiation [37] whilst this present study demonstrated that gedatolisib was the least effective agent at inhibiting the PI3K pathway during radiation treatment.

Our results clearly demonstrate the complexity of targeting the PI3K/AKT/MTOR pathway as this pathway is activated in cancers via several different mechanisms. These include amplification or mutational activation of genes encoding receptor tyrosine kinases, *RAS*, and/or the p110α catalytic subunit of PI3K (*PIK3CA*) and inactivation of the tumor suppressor gene, *PTEN*. In head and neck cancer, alteration in genes such as PTEN, TSC1 and PIK3CA encompass over 30% of the mutations found in this cancer [62–64]. In addition, loss of p53 function promotes mTORC1 activation and regulation of *PTEN* transcription [65]. In a previous study we have demonstrated that the UT-SCC-15 cell line harbored more variants in AKT1, AKT2, MTOR, PIK3CA, PIK3R1, PTEN and TP53 than the UT-SCC-14 cell line [37].

The results with dacomitinib were impressive and encouraging. Both tumor models, despite their different spectrum of mutations

**Table 3**
Quantitative analysis of immunoblotting data. The data was normalized to each actin control and then to the untreated control animal data and expressed as mean fold change.

| UT-SCC-14 | | | | | | | |
|---|---|---|---|---|---|---|---|
| | pEGFR | pMAPK | pPI3K | pAKT | pMTOR | p4EBP1 | pS6 |
| DAC | 0.12 | 0.57 | 0.82 | 0.80 | 0.74 | 0.22 | 1.01 |
| GED | 0.74 | 1.11 | 0.89 | 0.54 | 0.62 | 0.75 | 0.41 |
| DAC/GED | 0.40 | 0.84 | 1.06 | 0.48 | 0.93 | 1.02 | 0.88 |
| RT | 0.62 | 1.59 | 0.87 | 1.21 | 1.071 | 0.90 | 1.12 |
| DAC/RT | 0.03 | 0.62 | 0.59 | 0.42 | 0.92 | 0.27 | 0.87 |
| GED/RT | 0.47 | 1.52 | 0.78 | 0.68 | 0.83 | 0.83 | 0.80 |
| DAC/GED/RT | 0.029 | 0.512 | 0.72 | 0.29 | 0.48 | 0.58 | 0.16 |
| UT-SCC-15 | | | | | | | |
| DAC | 0.17 | 0.36 | 1.01 | 0.36 | 1.18 | 0.92 | 0.33 |
| GED | 1.32 | 0.64 | 0.91 | 0.45 | 0.43 | 0.52 | 0.39 |
| DAC/GED | 0.41 | 0.47 | 1.067 | 1.167 | 0.64 | 0.67 | 0.52 |
| RT | 1.2 | 0.79 | 0.84 | 1.09 | 0.54 | 1.03 | 1.02 |
| DAC/RT | 0.05 | 0.35 | 0.73 | 1.06 | 1.03 | 1.82 | 0.41 |
| GED/RT | 0.47 | 0.61 | 1.02 | 1.11 | 0.47 | 0.70 | 0.65 |
| DAC/GED/RT | 0.28 | 0.47 | 0.75 | 0.61 | 0.59 | 0.57 | 0.31 |

[37], were sensitive to drug alone and showed significant radiosensitization with 60% of UT-SCC-14 tumors and 100% of UT-SCC-15 tumors either with no detectable tumor or yet to meet sacrifice criteria, at the end of the pre-defined observation period, when the drug was combined with a clinically relevant fractionated radiation schedule. The in vitro data in this study adds to the comprehensive analysis of 27 different HNSCC cell lines by Ather et. al. [15] who showed that dacomitinib inhibited the growth of all head and neck cancer cell lines in a concentration-dependent manner. In our more limited series we also observed significant heterogeneity in $IC_{50}$ values that correlated with EGFR expression levels (Fig. 1). UT-SCC-14 with an $IC_{50}$ of 0.0023 μM was similar to most sensitive cell lines in the Ather study. The UT-SCC-15 cell line was the least sensitive in our study ($IC_{50}$ of 0.46 μM) but would still be classified as responsive using the Ather et al criteria of 1 μM. This present study takes the previous studies further by showing that dacomitinib produced a highly significant growth inhibition in the xenograft models of these cell lines (Table 2). The animal dosing of 10 mg/kg used in this study is similar to current use of 45 mg in recurrent HNSCC patients [66] and the schedule equivalent to 1 cycle of treatment for patients; the median number of cycles in patients is 4.

The striking data from this present study is the enhancement of the radiation response. Although dacomitinib did not radiosensitize in vitro (Fig. 2A and B), the effect *in vivo* was compelling. Our work validates and extends the research reported by Williams et al [16] who showed similar results in different HNSCC models and reported significant radiosensitization in FaDu-bearing xenografts. Our research extends these studies with a more clinically relevant combined schedule in low passage models of HNSCC that resulted in "tumor cure" in the mouse models. Based on this data it is somewhat disappointing that a Phase I dose escalation of dacomitinib in combination with standard cisplatin-based chemoradiation for locally advanced HNSCC was terminated early due to the uncertainty of the benefit of other HER-targeted therapies to platinum-based concurrent chemo-radiotherapy in other studies [67].

The conclusions from this study are that the combination of two agents targeting different nodes of the *EGFR/PI3K/AKT/mTOR* signaling pathway did not result in a greater inhibition of tumor growth, when combined with radiation, than the single most active agent. Dacomitinib was the most active agent and its activity, both alone, and in combination with radiation deserves further clinical consideration in locally advanced HNSCC.

## Declaration of Competing Interest

The authors declare that they have no known competing financial interests or personal relationships that could have appeared to influence the work reported in this paper.

## Acknowledgements

We acknowledge Dr. Reidar Grénman from the University of Turku, Finland for providing the UT-SCC cell lines. We acknowledge Pfizer for providing binimetinib and buparlisib.

## Funding source

Financial support was through internal research support.

## References

[1] Schlessinger J. Common and distinct elements in cellular signaling via EGF and FGF receptors. Science 2004;306(5701):1506–7.
[2] Hayes DN, Grandis J, El-Naggar AK. Comprehensive genomic characterization of squamous cell carcinoma of the head and neck in the Cancer Genome Atlas. In Proceedings of the 104th Annual Meeting of the American Association for Cancer Research. Washington, DC. Philadelphia (PA): AACR; Cancer Res; 2013.
[3] Stransky N, Egloff AM, Tward AD, et al. The mutational landscape of head and neck squamous cell carcinoma. Science 2011;333(6046):1157–60.
[4] Martin D, Abba MC, Molinolo AA, et al. The head and neck cancer cell oncogenome: a platform for the development of precision molecular therapies. Oncotarget 2014;5(19):8906–23.
[5] Iglesias-Bartolome R, Martin D, Gutkind JS. Exploiting the head and neck cancer oncogenome: widespread PI3K-mTOR pathway alterations and novel molecular targets. Cancer Discovery 2013;3:722–5.
[6] Freudlsperger C, Burnett JR, Friedman JA, Kannabiran VR, Chen Z, Van Waes C. EGFR–PI3K–AKT–mTOR signaling in head and neck squamous cell carcinomas: attractive targets for molecular-oriented therapy. Expert Opin Therap Targets 2011;15:63–74.
[7] Morris ZS, Harari PM. Interaction of radiation therapy with molecular targeted agents. JCO 2014;32:2886–93.
[8] Bonner JA, Harari PM, Giralt J, et al. Radiotherapy plus cetuximab for squamous-cell carcinoma of the head and neck. N Engl J Med 2006;354:567–78.
[9] Ang KK, Zhang Q, Rosenthal DI, et al. Randomized Phase III trial of concurrent accelerated radiation plus cisplatin with or without cetuximab for stage III to IV head and neck carcinoma: RTOG 0522. JCO 2014;32:2940–50.
[10] Taberna M, Oliva M, Mesía R. Cetuximab-Containing Combinations in Locally Advanced and Recurrent or Metastatic Head and Neck Squamous Cell Carcinoma. 2019;9:383.
[11] Wheeler DL, Huang S, Kruser TJ, et al. Mechanisms of acquired resistance to cetuximab: role of HER (ErbB) family members. Oncogene 2008;27:3944–56.
[12] Sok JC, Coppelli FM, Thomas SM, et al. Mutant epidermal growth factor receptor (EGFRvIII) contributes to head and neck cancer growth and resistance to EGFR targeting. Clin Cancer Res 2006;12:5064–73.

[13] Lièvre A, Bachet J-B, Le Corre D, et al. KRAS mutation status is predictive of response to cetuximab therapy in colorectal cancer. Cancer Res 2006;66:3992–5.
[14] Gonzales AJ, Hook KE, Althaus IW, et al. Antitumor activity and pharmacokinetic properties of PF-00299804, a second-generation irreversible pan-erbB receptor tyrosine kinase inhibitor. Mol Cancer Ther 2008;7:1880–9.
[15] Ather F, Hamidi H, Fejzo MS, et al. Dacomitinib, an irreversible Pan-ErbB inhibitor significantly abrogates growth in head and neck cancer models that exhibit low response to cetuximab. PLoS One. 2013;8:e56112.
[16] Williams JP, Kim I, Ito E, et al. Pre-clinical characterization of Dacomitinib (PF-00299804), an irreversible pan-ErbB inhibitor, combined with ionizing radiation for head and neck squamous cell carcinoma. PLoS One. 2014;9:e98557.
[17] Kim HS, Kwon HJ, Jung I, et al. Phase II Clinical and exploratory biomarker study of dacomitinib in patients with recurrent and/or metastatic squamous cell carcinoma of head and neck. Clin Cancer Res 2015;21:544–52.
[18] Horn D, Hess J, Freier K, Hoffmann J, Freudlsperger C. Targeting EGFR-PI3K-AKT-mTOR signaling enhances radiosensitivity in head and neck squamous cell carcinoma. Expert Opin Therap Targets 2015;19:795–805.
[19] Mohan S, Vander Broek R, Shah S, et al. MEK inhibitor PD-0325901 overcomes resistance to PI3K/mTOR inhibitor PF-5212384 and potentiates antitumor effects in human head and neck squamous cell carcinoma. Clin Cancer Res 2015;21:3946–56.
[20] Bussink J, van der Kogel AJ, Kaanders JH. Activation of the PI3-K/AKT pathway and implications for radioresistance mechanisms in head and neck cancer. Lancet Oncol 2008;9:288–96.
[21] Kim I-A, Bae S-S, Fernandes A, et al. Selective inhibition of Ras, phosphoinositide 3 Kinase, and Akt isoforms increases the radiosensitivity of human carcinoma cell lines. Cancer Res 2005;65:7902–10.
[22] Herzog A, Bian Y, Vander Broek R, et al. PI3K/mTOR Inhibitor PF-04691502 antitumor activity is enhanced with induction of wild-type TP53 in human xenograft and murine knockout models of head and neck cancer. Clin Cancer Res 2013;19:3808–19.
[23] Keysar SB, Astling DP, Anderson RT, et al. A patient tumor transplant model of squamous cell cancer identifies PI3K inhibitors as candidate therapeutics in defined molecular bins. Mol Oncol. 2013;7:776-90.
[24] Chang K-Y, Tsai S-Y, Wu C-M, Yen C-J, Chuang B-F, Chang J-Y. Novel phosphoinositide 3-Kinase/mTOR dual inhibitor, NVP-BGT226, displays potent growth-inhibitory activity against human head and neck cancer cells in vitro and in vivo. Clin Cancer Res 2011;17:7116–26.
[25] D'Amato V, Rosa R, D'Amato C, et al. The dual PI3K/mTOR inhibitor PKI-587 enhances sensitivity to cetuximab in EGFR-resistant human head and neck cancer models. Br J Cancer 2014;110:2887–95.
[26] Mazumdar T, Byers LA, Ng PK, et al. A comprehensive evaluation of biomarkers predictive of response to PI3K inhibitors and of resistance mechanisms in head and neck squamous cell carcinoma. Mol Cancer Ther 2014;13:2738–50.
[27] Leiker AJ, DeGraff W, Choudhuri R, et al. Radiation enhancement of head and neck squamous cell carcinoma by the dual PI3K/mTOR inhibitor PF-05212384. Clin Cancer Res 2015;21:2792–801.
[28] Lattanzio L, Tonissi F, Monteverde M, et al. Treatment effect of buparlisib, cetuximab and irradiation in wild-type or PI3KCA-mutated head and neck cancer cell lines. Invest New Drugs 2015;33:310–20.
[29] Mallon R, Feldberg LR, Lucas J, et al. Antitumor Efficacy of PKI-587, a Highly Potent Dual PI3K/mTOR Kinase Inhibitor. Clin Cancer Res 2011;17:3193–203.
[30] Kiuru A, Servomaa K, Grénman R, Pulkkinen J, Rytömaa T. p53 mutations in human head and neck cancer cell lines. Acta Otolaryngol 1997;529:237–40.
[31] Jääskelä-Saari HA, Kairemo KJA, Ramsay HA, Grénman R. Squamous cell cancer cell lines: sensitivity to bleomycin and suitability for animal xenograft studies. Acta Otolaryngol 1997;529:241–4.
[32] Wobb J, Krueger SA, Kane JL, et al. The effects of pulsed radiation therapy on tumor oxygenation in 2 murine models of head and neck squamous cell carcinoma. Int J Radiat Oncol Biol Phys 2015;92:820–8.
[33] Wilson GD, Thibodeau BJ, Fortier LE, et al. Cancer stem cell signaling during repopulation in head and neck cancer. Stem Cells Int 2016;2016:1894782.
[34] Wilson GD, Thibodeau BJ, Fortier LE, et al. Glucose metabolism gene expression patterns and tumor uptake of 18F-fluorodeoxyglucose after radiation treatment. Int J Radiat Oncol Biol Phys 2014;90:620–7.
[35] Wilson GD, Thibodeau BJ, Fortier LE, et al. Gene expression changes during repopulation in a head and neck cancer xenograft. Radiother Oncol 2014;113:139–45.
[36] Wilson GD, Marples B, Galoforo S, et al. Isolation and genomic characterization of stem cells in head and neck cancer: stem cells in head and neck cancer. Head Neck 2013;35:1573–82.
[37] Tonlaar N, Galoforo S, Thibodeau BJ, et al. Antitumor activity of the dual PI3K/MTOR inhibitor, PF-04691502, in combination with radiation in head and neck cancer. Radiother Oncol 2017;124:504–12.
[38] Meyer K, Krueger SA, Kane JL, et al. Pulsed radiation therapy with concurrent cisplatin results in superior tumor growth delay in a head and neck squamous cell carcinoma murine model. Int J Radiat Oncol Biol Phys 2016;96:161–9.
[39] Kane JL, Krueger SA, Hanna A, et al. Effect of irradiation on tumor microenvironment and bone marrow cell migration in a preclinical tumor model. Int J Radiat Oncol Biol Phys 2016;96:170–8.
[40] Huang J, Chunta JL, Amin M, et al. Detailed characterization of the early response of head-neck cancer xenografts to irradiation using 18F-FDG-PET imaging. Int J Radiat Oncol Biol Phys 2012;84:485–91.
[41] Huang J, Chunta JL, Amin M, et al. Early treatment response monitoring using 2-deoxy-2-[ 18 F]fluoro-D-glucose positron emission tomography imaging during fractionated radiotherapy of head neck cancer xenografts. Biomed Res Int 2014;2014:598052.
[42] Blas K, Wilson TG, Tonlaar N, Galoforo S, Hana A, Marples B, Wilson GD. Dual blockade of PI3K and MEK in combination with radiation in head and neck cancer. Clin Transl Radiat Oncol 2018;11:1–10.
[43] Baschnagel AM, Galoforo S, Thibodeau BJ, et al. Crizotinib fails to enhance the effect of radiation in head and neck squamous cell carcinoma xenografts. Anticancer Res 2015;35:5973–82.
[44] Zips D, Böke S, Kroeber T, et al. Prognostic value of radiobiological hypoxia during fractionated irradiation for local tumor control. Strahlenther Onkol 2011;187:306–10.
[45] Yaromina A, Zips D, Thames HD, et al. Pimonidazole labelling and response to fractionated irradiation of five human squamous cell carcinoma (hSCC) lines in nude mice: the need for a multivariate approach in biomarker studies. Radiother Oncol 2006;81:122–9.
[46] Yaromina A, Thames H, Zhou X, et al. Radiobiological hypoxia, histological parameters of tumour microenvironment and local tumour control after fractionated irradiation. Radiother Oncol 2010;96:116–22.
[47] Yaromina A, Krause M, Thames H, et al. Pre-treatment number of clonogenic cells and their radiosensitivity are major determinants of local tumour control after fractionated irradiation. Radiother Oncol 2007;83:304–10.
[48] Gurtner K, Ebert N, Pfitzmann D, et al. Effect of combined irradiation and EGFR/Erb-B inhibition with BIBW 2992 on proliferation and tumour cure in cell lines and xenografts. Radiat Oncol 2014;9:261.
[49] Eicheler W, Zips D, Dörfler A, Grénman R, Baumann M. Splicing mutations in TP53 in human squamous cell carcinoma lines influence immunohistochemical detection. J Histochem Cytochem 2002;50:197–204.
[50] Eicheler W, Krause M, Hessel F, Zips D, Baumann M. Kinetics of EGFR expression during fractionated irradiation varies between different human squamous cell carcinoma lines in nude mice. Radiother Oncol 2005;76:151–6.
[51] Anisuzzaman ASM, Haque A, Wang D, et al. In vitro and in vivo synergistic antitumor activity of the combination of BKM120 and erlotinib in head and neck cancer: mechanism of apoptosis and resistance. Mol Cancer Ther 2017;16:729–38.
[52] Michmerhuizen NL, Leonard E, Kulkarni A, Brenner JC. Differential compensation mechanisms define resistance to PI3K inhibitors in PIK3CA amplified HNSCC. Otorhinolaryngol Head Neck Surg. 2016;1:44-50.
[53] Michmerhuizen NL, Leonard E, Matovina C, et al. Rationale for using irreversible epidermal growth factor receptor inhibitors in combination with phosphatidylinositol 3-kinase inhibitors for advanced head and neck squamous cell carcinoma. Mol Pharmacol 2019;95:528–36.
[54] Rebucci M, Peixoto P, Dewitte A, et al. Mechanisms underlying resistance to cetuximab in the HNSCC cell line: role of AKT inhibition in bypassing this resistance. Int J Oncol. 2011;38:189–200.
[55] Silva-Oliveira RJ, Melendez M, Martinho O, et al. AKT can modulate the in vitro response of HNSCC cells to irreversible EGFR inhibitors. Oncotarget 2017;8:53288–301.
[56] Young NR, Liu J, Pierce C, et al. Molecular phenotype predicts sensitivity of squamous cell carcinoma of the head and neck to epidermal growth factor receptor inhibition. Mol Oncol. 2013;7:359-68.
[57] Young NR, Soneru C, Liu J, et al. Afatinib efficacy against squamous cell carcinoma of the head and neck cell lines in vitro and in vivo. Targ Oncol 2015;10:501–8.
[58] Engelman JA, Luo Ji, Cantley LC. The evolution of phosphatidylinositol 3-kinases as regulators of growth and metabolism. Nat Rev Genet 2006;7:606–19.
[59] O'Reilly KE, Rojo F, She Q-B, et al. mTOR inhibition induces upstream receptor tyrosine kinase signaling and activates Akt. Cancer Res 2006;66:1500–8.
[60] Serra V, Markman B, Scaltriti M, et al. NVP-BEZ235, a Dual PI3K/mTOR Inhibitor, Prevents PI3K Signaling and inhibits the growth of cancer cells with activating PI3K mutations. Cancer Res 2008;68:8022–30.
[61] Wallin JJ, Edgar KA, Guan J, et al. GDC-0980 Is a Novel Class I PI3K/mTOR kinase inhibitor with robust activity in cancer models driven by the PI3K pathway. Mol Cancer Ther 2011;10:2426–36.
[62] Qiu W, Schonleben F, Li X, et al. PIK3CA mutations in head and neck squamous cell carcinoma. Clin Cancer Res. 2006;12:1441–6.
[63] Lui VWY, Hedberg ML, Li H, et al. Frequent mutation of the PI3K pathway in head and neck cancer defines predictive biomarkers. Cancer Discovery 2013;3:761–9.
[64] Agrawal N, Frederick MJ, Pickering CR, et al. Exome sequencing of head and neck squamous cell carcinoma reveals inactivating mutations in NOTCH1. Science 2011;333:1154–7.
[65] Stambolic V, MacPherson D, Sas D, et al. Regulation of PTEN Transcription by p53. Mol Cell 2001;8:317–25.
[66] Abdul Razak AR, Soulières D, Laurie SA, et al. A phase II trial of dacomitinib, an oral pan-human EGF receptor (HER) inhibitor, as first-line treatment in recurrent and/or metastatic squamous-cell carcinoma of the head and neck. Ann Oncol 2013;24:761–9.
[67] Prawira A, Brana-Garcia I, Spreafico A, et al. Phase I trial of dacomitinib, a pan-human epidermal growth factor receptor (HER) inhibitor, with concurrent radiotherapy and cisplatin in patients with locoregionally advanced squamous cell carcinoma of the head and neck (XDC-001). Invest New Drugs 2016;34:575–83.